

TEMPERATURES IN A HEATED AIR JET DISCHARGED DOWNWARD

R. A. SEBAN,* M. M. BEHNIA† and K. E. ABRFU†
 College of Engineering, University of California at Berkeley,
 Berkeley, CA 94720, U.S.A.

(Received 15 September 1977 and in revised form 13 March 1978)

Abstract—Measurements of temperature in a heated turbulent air jet discharged downward into an ambient air environment show that centerline temperatures and the penetration depth are predicted adequately by constant property theories for the downward flow alone. The radial temperature profiles and the estimates of the breadth of the downward jet indicate that the upward flow does influence the downward flow and that the satisfactory predictions that are obtained may be a coincidence.

NOMENCLATURE

- b , radial location where u/u_c is $1/e$;
 b_i , radial location where $\Delta T/\Delta T_c$ is $1/e$;
 g , gravity acceleration;
 G_0 , inverse of the square of the Froude number, $G_0 = r_0 g \beta \Delta T_0 / u_0^2$;
 r , radius from centerline;
 r_1 , radius to indicated position of zero velocity;
 r_∞ , radius to location where $\Delta T = 1^\circ\text{C}$;
 ΔT , excess of local temperature above the ambient;
 u , velocity;
 u_u, u_d , average upward and downward velocities from energy balance;
 x , distance measured downward from nozzle exit plane;
 x_1 , penetration depth of the jet;

Greek symbols

- α , entrainment coefficient;
 β , coefficient of cubical expansion;
 λ , ratio, b_i/b .

Subscripts

- c , centreline;
 e , at location of first Gaussian profiles;
 m , mean value;
 0 , at the nozzle outlet.

INTRODUCTION

WHEN a jet of heated fluid is discharged downward into an ambient region of the same fluid the negative buoyancy decelerates the jet flow and this ultimately reverses to produce an upward flow surrounding the central, downward flow. The specification of the temperature and velocity distributions, and the depth of penetration, of such a flow is basically an elliptical problem which has not yet been solved. Solutions of the parabolic problem in which the upward, return, flow is ignored, have been obtained by integral me-

thods by a number of investigators [1–3] and these results all indicate that the flow is little affected by buoyancy until near the termination of the central flow, when the velocity, being then sufficiently reduced, approaches zero rapidly. The theories predict a penetration depth in terms of the distance to the point of zero downward velocity on the jet centerline.

Turner [4, 5] measured the penetration distance of salt water injected upward into fresh water, and obtained penetration heights compatible with these analytical predictions.

As a further appraisal of this situation, centerline temperatures have been measured for a jet of air discharged downward into ambient air, and comparisons can be made from them that show good correspondence with the theory up to the point of maximum penetration as exhibited by the rapid drop in centerline temperature. Some radial temperature distributions are also shown; these disagree with the theory and imply a substantial influence of the upward, return flow in a way not yet explained, to the extent that the degree of correspondence that is obtained with the theory appears to be coincidental. These results, which follow, are preceded by a brief review of the theory.

THEORY

The integral theories take Gaussian distribution of velocity, $u = u_c e^{-(r/b)^2}$ and of temperature $\Delta T = \Delta T_c e^{-(r/b)^2}$, and limit the variation of density to the buoyant force term, so that the equations of continuity, momentum, and energy become:

$$\frac{d(u_c b^2)}{dx} = 2 \alpha u_c b$$

$$\frac{d(u_c^2 b^2)}{dx} = 2 \lambda^2 b^2 g \beta \Delta T_c$$

$$\frac{d}{dx} \left[\frac{\lambda^2}{2(1 + \lambda^2)} u_c b^2 g \beta \Delta T_c \right] = 0 \quad (1)$$

where

$$\Delta T_c = T_c - T_\infty, \lambda = b_i/b.$$

Morton solved these equations for initial conditions of

* Professor of mechanical engineering.

† Research assistant.

a point source, for which, at $x = 0$, the momentum, $(u_c^2 b^2)_0$, and the energy, $(\lambda^2 b^2 u_c g \beta \Delta T)_0$, are prescribed and the mass flow rate, $(u_c b^2)_0$, is zero. The velocity is found to become zero at the point

$$x_1 = \frac{1.454}{2^{3/2} \alpha^{1/2} \lambda} \frac{(u_c b)_0^{3/2}}{(u_c b q \beta \Delta T_0)^{1/2}}. \quad (2)$$

This result can be related approximately to the flow from a small infinite jet with uniform velocity, u_0 , and temperature, ΔT_0 , by balancing the momentum rates, so that $b_0 = 2^{1/2} r_0$, and the energy rates, so that $\Delta T_{c0} = \Delta T_0 (1 + \lambda^2) / 2\lambda^2$. Then

$$\frac{x_1}{r_0} = \left(\frac{1.454}{2^{3/2} \alpha^{1/2} \lambda} \right) (2^{1/4}) \left(\frac{2\lambda^2}{1 + \lambda^2} \right)^{1/2} \frac{1}{G_0^{1/2}} \quad (3)$$

where

$$G_0 = \frac{r_0 g \beta \Delta T_0}{u_0^2}.$$

For the situation of a finite source, for which the mass flow, momentum rate, and energy rate are prescribed from the uniform velocity and temperatures that exist there, there is a region of flow development at the end of which the profiles are presumed to be Gaussian, and which region is defined by a separate and more approximate entrainment specification for this region. Its specification enables the definition of a virtual origin which would yield the Gaussian profiles at the end of the region, and Abraham [3] indicated that this origin was located upstream of the nozzle when the buoyancy opposed the flow, and was dependent in distance on the relative buoyancy parameter, G_0 , never being more than 10 radii upstream even for the greatest buoyancy, and for most practical cases being much less. Morton [2] matched his result for the point source with that of a finite source from which the discharge profiles were Gaussian, and showed a downstream displacement of the virtual origin, increasing as G_0 increased.

Turner [4] made measurements of the penetration height of salt water injected upward into fresh water and deduced the height as

$$\frac{x_1}{r_0} = 2.46 \frac{1}{G_0^{1/2}}. \quad (4)$$

This is the form of equation (3) and implies a virtual origin close to the discharge location. For the small values of G_0 this is indicated by both Abraham and by Morton. For G_0 as large as 0.64, Abraham indicates an origin at about $x/r_0 = -5$, and Morton a larger positive value. Turner's penetration depths scatter substantially, but indicate a trend like that indicated by Abraham. However, the error in using equation 4 is small and equation (3) is therefore indicated to be appropriate; for $\alpha = 0.055$, $\lambda = 1.1$, it indicates a coefficient of 2.52, and for $\lambda = 1.0$ a coefficient of 2.60. The former, associated with values considered to be typical of a non-buoyant jet, is close to Turner's experimental value.

The centerline temperature given by the Morton analysis varies almost linearly, as for the non-buoyant jet, to a distance that is about 86% of that given by equation (3). Thereafter the jet begins to broaden rapidly and the centerline temperature remains almost constant. In the non-buoyant jet, with $\lambda = 1$, beginning with a Gaussian profile at x_e/r_0 , the temperature ratio is $\Delta T_c = \Delta T_0 [1 + 2^{1/2} \alpha (x - x_e/r_0)]^{-1}$ and the width b is $b = 2^{1/2} [1 + 2^{1/2} \alpha (x - x_e/r_0)]$.

In the present experiments the temperature of the air issuing from the jet was high enough to make the density variation substantial and this affects comparisons with the foregoing theory which, for Gaussian profiles, cannot readily account for variable density. Density changes can be accounted for if the profiles of velocity and temperatures are taken to be uniform (the "top hat" profiles). If this is done, neglecting buoyancy, the consequent jet result for the largest density difference of the present experiments gives value of $\Delta T_c/\Delta T_0$ at a given distance that are no more than 10% different from the result for constant density. This implies that the present results can be compared to the foregoing theory in which the variable density is accounted for only in the buoyancy term.

Equation (1) can, of course, also be solved numerically, beginning with Gaussian profiles as they are realized from uniform jet outlet conditions via a postulate about the entrainment conditions in the region in which the Gaussian profiles develop. This permits the prescription of a variable entrainment coefficient, if desired. With a constant coefficient, the result is essentially the same as that of Morton, giving a region in which the temperature decreases as for the non-buoyant jet, followed by a short region in which the profiles broaden rapidly and the temperature remains essentially constant.

MEASUREMENTS

Hot air jets, produced by the heater-plenum unit described previously in [6] issued downward from either 1.15 or 0.5 cm radius nozzles located approximately centrally in a 1.2 m square enclosure, the level of the outlet being 1.5 m above the floor, where there was a circumferential ventilation slot 8 cm high. The enclosure rose 1.7 m from the floor. A top closure, 0.64 m high, could be placed above this enclosure, with a 4 cm ventilation slot at the joint.

The mean flow was metered but the energy addition to the air was unknown, and was inferred from temperature traverses made across the nozzle exit. Neither the velocity or temperature profiles across the exit plane were uniform, decreasing at the edges from relatively uniform values across the central region. Thus the energy rate, taken as the product of the mass flow and the average exit temperature, ΔT_{0m} , was high, but this excess was estimated to be no more than 5%.

Temperatures were obtained both on the centerline and radially, and were indicated on a chart recorder. Particularly in the region away from the centerline, the temperature fluctuations were large and mean values were obtained by averaging the record.

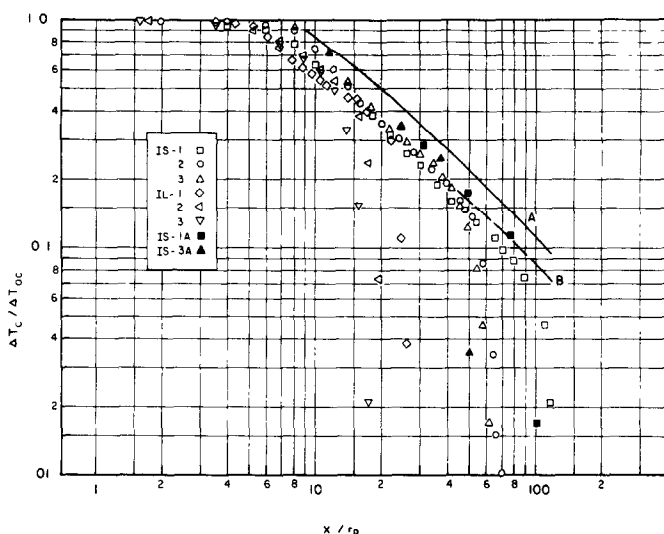


FIG. 1. Centerline temperatures. Operating conditions are in Table 1. Curve A is the prediction for a non-buoyant jet, Curve B is that reduced by 30%.

CENTERLINE TEMPERATURES

Centerline temperatures were obtained primarily with the top of the enclosure in place and these are shown by the open symbols on Fig. 1 as the ratio of the excess over ambient at a location x/r_0 , to that at the nozzle exit. Three runs are shown for both the large and the small nozzles, and the operating conditions are given on Table 1. The temperature ratio shown on Fig. 1 is constant in the immediate region downstream of the nozzle, then begins to decrease as the influence of the shear layer reaches the centerline. Then there is an almost linear decrease in the temperature ratio to a point at which, depending upon the value of G_0 , it falls rapidly. This is the terminal region of the downward flow. For reference, there is shown a prediction for a non-buoyant jet for $\lambda = 1.1$ and $\alpha = 0.55$ with first Gaussian profiles at $x_c/r = 9$. This is 30% higher than a line through the data, and this is of the order of the effect of the actual value of $\Delta T_{0c}/\Delta T_{0m}$ and of the error in the energy rate. This confirms the theoretical indication of an initial

region of performance that is like that of a non-buoyant jet.

When the top of the enclosure was removed the temperature ratios increased. For this condition only a few points were obtained and these are shown as solid points, which are about 15% higher than the values indicated for the situation with the top in place. As noted for the upward jet as described in [6], there is an effect of the enclosure, but it is for the downward jet opposite to that for the upward jet.

MAXIMUM DEPTH

The temperature ratio decreases rapidly at the maximum depth and it becomes practically asymptotic to a line of given x/r_0 and this distance is shown by the square points on Fig. 2, as a function of the buoyancy parameter G_0 .

It is hard to judge, from the experimental data, the location of the initiation of the significant departure of the centerline temperatures from the expectation for a non-buoyant jet. Estimates of a 10% departure from

Table 1. Operating conditions

	$\frac{u_{0m}r_0}{v_0}$	r_0 cm	u_{0m} cm/s	ΔT_{0m} °C	T_{0c} °C	$\frac{\Delta T_{0c}}{\Delta T_{0m}}$	$G_0 \times 10^4$
IS-1	1770	0.5	9.33	240	180	1.33	3.5
2	1033	0.5	6.1	320	243	1.32	10.7
3	1923	0.5	5.7	321	267	1.20	14.0
IL-1	1130	1.15	2.11	117	97	1.21	97
2	894	1.15	2.03	209	182	1.15	116
3	770	1.15	1.78	235	191	1.23	227
IS-1A	1778	0.5	9.85	238	211	1.13	3.6
IS-3A	922	0.5	5.78	320	278	1.15	14.0

T_∞ was about 26°C.

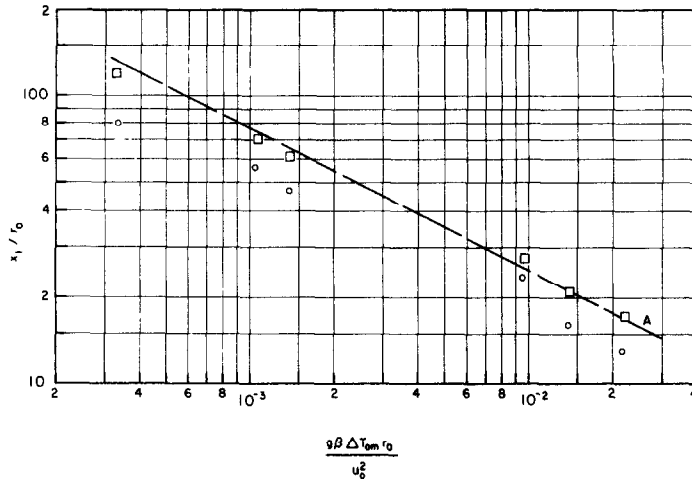


FIG. 2. Penetration distances. Squares are experimental distances, circles are distances to 10% temperature departure, Curve A is equation (3).

the prior trend of the temperatures give the circle points shown on Fig. 2. It is between these locations and the maximum depth that the central flow is decelerated to turn upward again.

A line on Fig. 2 shows Turner's result, in good accordance with the present estimate of maximum depth. As already indicated, this is near the indication of equation (3) with $\alpha = 0.055$ and $\lambda = 1.1$. If Turner's result is reduced to 0.86 of that value, the prior estimate for the region of departure from buoyant jet performance, it is substantially above the circles on Fig. 2 which are of the order of 0.75 of the terminal value.

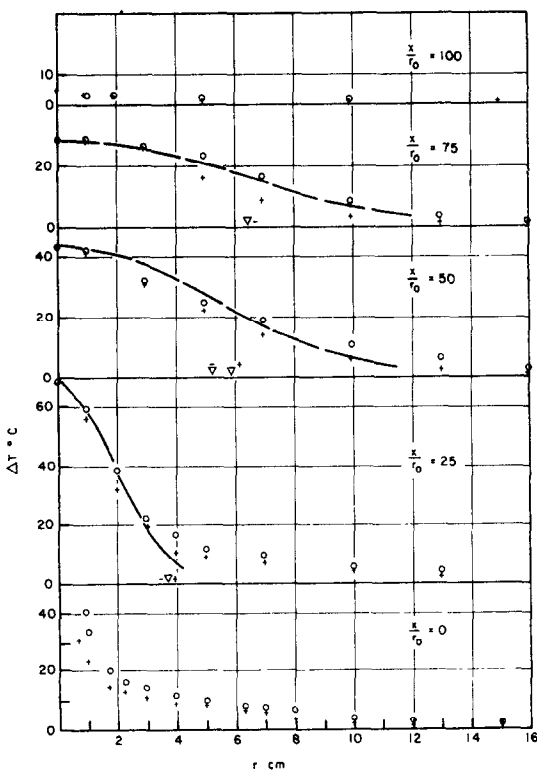


FIG. 3. Radial temperatures for run IS-1A. The triangles indicate abscissas for the limit of downward flow.

RADIAL TEMPERATURE PROFILES

Radial temperature profiles were taken mainly with the top of the enclosure removed, and the solid points on Fig. 1 correspond to this condition. They were obtained only with smaller nozzle, for Runs IS-1A and IS-3A, with the results that are shown in Figs. 3 and 4.

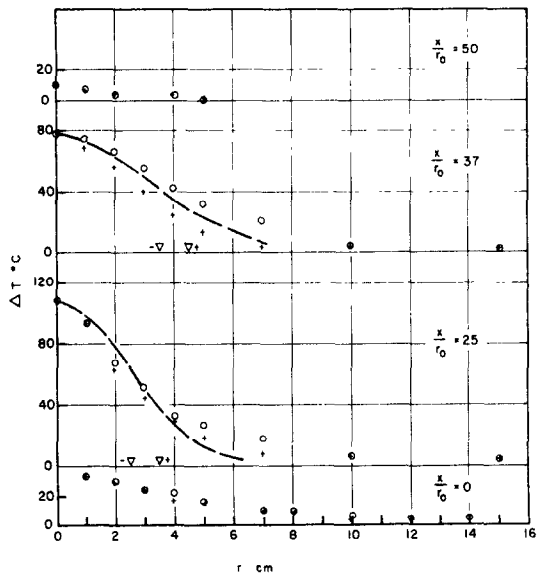


FIG. 4. Radial temperatures for run IS-3A.

The symbols of the circle and the plus refer to the two directions from the centerline in the single vertical traverse plane that was used, and the profiles reveal considerable asymmetry, consistent in that the plus side always gave lower temperatures, but not consistent as to the degree of asymmetry at the various depths below the nozzle. The profiles on each side could be fitted fairly to a Gaussian curve, defining b , at $\Delta T/\Delta T_c = 1/e$, but on the figures there are shown the curves corresponding to the average value of b , obtained from the fit of the separate sides of the profiles. These values of b , are contained in Table 2 and are compared there to the values associated with the

Table 2.

	$\frac{x}{r_0}$	IS-1A				IS-3A			
		0	26	50	75	0	12	25	37
b_i expt	cm		2.5	7	8.35			3.3	4.5
b_i jet	cm		1.75	3.24	5.1			1.8	2.6
r_i	cm		3.5	5.6	6.5		2.5	3.0	4.0
r_∞	cm	23	25	32	20	25		35	35
u_d	cm/s	985	90	38	34	578		42	29
u_u	cm/s	28	30	12	28	11		6	10

non-buoyant jet with a Gaussian profile beginning at $x_0/r_0 = 9$, which corresponds to what has been considered as a basis for reasonable prediction of the temperatures. There is no correspondence at all, for the values of b_i far exceed the values associated with the jet, which was presumed to approximate reasonably the flow for $x/r_0 < 80$ for IS-1A and $x/r_0 < 45$ for IS-3A.

In an effort to define the limit of the downward flow a direction indicator made of a thin paper rectangle 2.5 cm long in the radial direction and 1 cm wide was attached to a transverse rod by a slender paper section and supported by wire from below, so that in the downward flow the paper would be held against the support and in upward flow the paper would rise above the support. The large area of the indicator was necessary to get a consistent response, but that response was made intrinsically undefinable because of the unknown nature of the velocity variation near the edge of the central flow. However, by traversing the indicator, positive indications of upward or downward flow were obtained within an interval of about 1 cm, and the mean of these values is shown on Figs. 3 and 4 for the plus and minus sides of the flow, a high radius usually being indicated for the plus side. The average of these values is indicated as r_i in Table 2. It is in this region also that there occur the maximum fluctuations in the temperature.

If these values of r_i indicate even approximately the radial distances to which the downward flow extends, then there is a coincidence in the prediction of the centerline temperature and the penetration depth by the analysis which ignores the upward flow and uses an entrainment coefficient associated with a non-buoyant jet.

No adequate definition is possible for the outer extent of the upward flow, though a radius specified on the basis of a given temperature ratio might be appropriate. The data does not allow this appraisal, and it would be insensitive in any case, for the temperature profiles are flat and extend far beyond the maximum radii that are shown on Figs. 3 and 4. To give some kind of indication, there are contained in Table 1 the average distances, r_∞ , to the point at which the excess temperature over ambient was about 1°C. These are greater at greater depth, and are smaller toward the nozzle plane, where the indication for both runs was for r_∞ about 25 cm.

Turner [4, 5] presented a sketch, which is a com-

posite of photographs showing the radial extent of the (ostensibly dyed) salt water, for one case of his experiments, which by scaling from the sketch, corresponds to a relative penetration x_1/r_0 of about 56, and this is somewhat similar to run IS-3A. The visibility of the flow in Turner's experiment must have corresponded to some fixed excess concentration, so that this might be consistent with the excess temperature that was used to define r_∞ in the present experiments.

For his run, Turner indicates an almost constant value of $r_\infty/r_0 = 13$ and this is far less than the values of $50 < r_\infty/r_0 < 70$ that are indicated in Table 2 for IL-3A. In this respect, the value of temperature difference at $r/r_0 = 13$ gives, for run IL-3A, the values 11°, 10°, 13° at $x/r_0 = 0, 25$ and 37. These values too are relatively constant, and it might be inferred that Turner's photography did not reveal concentrations sufficiently low to define the true extent of his downward flow. (This would not be so important in the specification of x_1/r_0 , in view of the steep gradients that exist there.)

Turner's picture reveals a rounded top extending downward from $x_1/r_0 = 56$ to $x/r_0 = 40$, this being $0.67 x_1/r_0$. Run IS-3 indicates $x_1/r_0 = 60$ and the location of 10% temperature departure at $x/r_0 = 46$, this being $0.71 x_1/r_0$, so that a location of this order is indicated as the beginning of the turning of the flow.

A few measurements of radial temperatures and radius r_i were made for the situation with the top of the enclosure in place, the condition for which the detailed centerline temperatures were obtained. The aspects of the results are the same as those shown on Figs. 3 and 4, with temperatures on the negative side being higher than those on the positive side but, in what appears to be inconsistent, the values of b_i were slightly lower while those for r_i were greater. The increased width is consistent, at least, with the slightly lower centerline temperatures that were observed for this mode of operation.

Little more can be done with these radial profiles of temperatures in the absence of knowledge about the velocity profiles, but, as an indication of magnitudes, uniform velocities were assumed for the downward and upward flows and with this assumption, and the actual temperature profiles, and the assumption of constant and equal energy flow in the downward and upward flows, the velocities were calculated as u_d and u_u . These

are indicated in Table 2. Because r_i is indicated to be larger than would be expected from any appraisal related to a jet, the values of u_d are much smaller than the average velocity for a jet flow. The upward velocity is significant, but its magnitude is uncertain because of the error in ascertaining the outer radius r_∞ . The effect of buoyancy would be to accelerate this flow, but the results for u_u are somewhat inconclusive in this respect, they show a minimum in u_u in the region in which the thermal behavior departs from the jet-like behavior, as shown on Fig. 1, and then the velocity u_u does show higher values near the nozzle exit plane.

With this model, there should be, at r_i , gradient transport of heat into the upward flow, and convection of heat into the downward flow. Unless these balance exactly, the energy in the streams will not be constant at the value that emerges from the jet, and the values of u_d and u_i will be different than those in Table 2.

CONCLUSIONS

Measured centerline temperatures in a heated air jet discharged downward into ambient air support the analytical deduction that these are predictable from the theory for a non-buoyant jet up to a final region for which the theory indicates a relatively constant final temperature but where actually the temperature de-

creases rapidly as the flow is reversed. This same theory gives appropriate values of the penetration depth.

Radial temperature measurements reveal wide profiles that extend significantly into the region of upward flow, and it is probable that the width of the downward flow is greater than that implied theoretically. This implies a substantial interaction between the downward and upward flow and suggests as a possible coincidence the predictability of centerline temperature and jet penetration by the simple theory that neglects the outer flow.

REFERENCES

1. C. H. Priestley and T. K. Ball, Continuous convection from an isolated source of heat, *Q. Jl R. Met. Soc.* **81**, 144-157 (1955).
2. B. R. Morton, Forced plumes, *J. Fluid Mech.* **5**, 151-163 (1959).
3. G. Abraham, Jet diffusion in stagnant ambient fluid, Delft Hydraulics Laboratory, Pub. No. 29 (1963).
4. J. S. Turner, Jets and plumes with negative or reversing buoyancy, *J. Fluid Mech.* **26**, 779-792 (1966).
5. J. S. Turner, *Buoyancy Effects in Fluids*. Cambridge University Press, Cambridge (1973).
6. R. A. Seban and M. M. Behnia, Turbulent buoyant jets in unstratified surroundings, *Int. J. Heat Mass Transfer* **19**, 1176-1204 (1976).

TEMPERATURE DANS UN JET DESCENDANT D'AIR CHAUD

Résumé—Des mesures de température dans un jet turbulent d'air chaud débouchant dans un environnement d'air ambiant montrent que les températures sur l'axe et la profondeur de pénétration sont estimées correctement par des théories à propriétés constantes seulement pour l'écoulement descendant. Les profils radiaux de température et l'estimation de la largeur du jet descendant montrent que le jet ascendant influence le premier et que les prévisions satisfaisantes obtenues peuvent être une coincidence.

TEMPERATUREN IN EINEM BEHEIZTEN, NACH UNTEN AUSGEBLASENEN LUFTSTROM

Zusammenfassung—Messungen der Temperatur einer beheizten turbulenten Luftströmung aus einer nach unten in die Umgebungsluft gerichteten Düse zeigen, daß die Temperatur in der Strömungs-Mittelachse und die Eindringtiefe sich für konstante Eigenschaften für die Abwärtsströmung allein theoretisch berechnen lassen. Das radiale Temperaturprofil und die geschätzte Breite des abwärts gerichteten Luftstrahls weisen daraufhin, daß die Aufwärtsströmung die Abwärtsströmung beeinflusst und daß die zufriedenstellende Übereinstimmung mit Rechenergebnissen zufällig sein könnte.

ТЕМПЕРАТУРНОЕ ПОЛЕ НАГРЕТОЙ ИСТЕКАЮЩЕЙ ВНИЗ СТРУИ ВОЗДУХА

Аннотация — Измеренные значения температуры нагретой турбулентной струи воздуха, истекающей вниз в окружающий объем воздуха, показывают, что температура по оси струи и глубина проникновения хорошо рассчитываются с помощью теории постоянства свойств только в случае направленной вниз струи. Радиальные профили температуры и оценки ширины падающей струи свидетельствуют о влиянии встречного потока воздуха, а также о том, что удовлетворительное совпадение с расчётными значениями могло оказаться случайным.